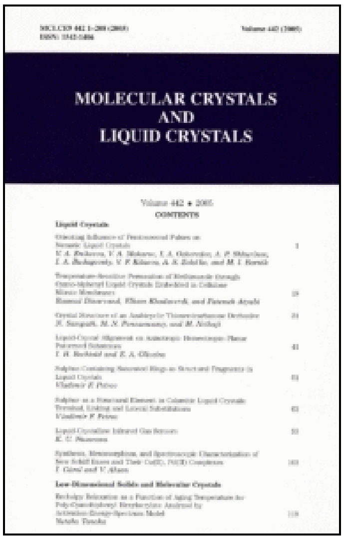
MOLECULAR CRYSTALS
AND
LIQUID CRYSTALS

Molecular Crystals and Liquid Crystals
Publication details, including instructions for authors and subscription information:
http://www.informaworld.com/smpp/title~content=t713644168

Shear-Induced Reorientation in a Tumbling Type Nematic Hybrid-Oriented Film

A. V. Zakharov[a]; A. A. Vakulenko[a]
[a] Saint Petersburg Institute for Machine Sciences, the Russian Academy of Sciences, Saint Petersburg, Russia

First published on: 13 July 2010

To cite this Article Zakharov, A. V. and Vakulenko, A. A.(2010) 'Shear-Induced Reorientation in a Tumbling Type Nematic Hybrid-Oriented Film', Molecular Crystals and Liquid Crystals, 525: 1, 194 — 203
To link to this Article: DOI: 10.1080/15421401003799771
URL: http://dx.doi.org/10.1080/15421401003799771

Mol. Cryst. Liq. Cryst., Vol. 525: pp. 194–203, 2010

ISSN: 1542-1406 print/1563-5287 online
DOI: 10.1080/15421401003799771

Taylor & Francis
Taylor & Francis Group

Shear-Induced Reorientation in a Tumbling Type Nematic Hybrid-Oriented Film

A. V. ZAKHAROV AND A. A. VAKULENKO

Saint Petersburg Institute for Machine Sciences, the Russian Academy of Sciences, Saint Petersburg, Russia

It has been shown the simple way, in the framework of the classical Ericksen-Leslie theory, together with accounting for the thermoconductivity equation for the temperature field, how a temperature gradient across a tumbling type hybrid-oriented liquid crystalline film, such as 4-cyano-4′-octylbiphenyl, may set up under action of a shear stress (SS). It has also been shown that the temperature difference on the restricted surfaces, which initially was equal to zero, is proportional to the heat flow, for instance, across the upper restricted surface, when the temperature on the lower surface is kept constant, and grows up to several degrees, under influence of the SS effort directed both in the positive and negative directions.

Keywords Liquid crystal; thermomechanical stress

PACS 61.30.-v; 47.57.Lj; 65.40.De

Introduction

The widely used flat-panel liquid crystal displays (LCDs) consist of a liquid crystal (LC) film sandwiched between two glass or plastic surfaces on scale of the order of micrometers across which a voltage may be applied, independently to each pixel of the LCD. This applied electric field may alter the molecular configuration of the LC layer and thus alter the optical characteristics of the LCD. In the field of LC phases, a great deal is known about their deformations under influence of electric or magnetic fields [1], whereas, on the other hand, comparatively little is known about effect of a temperature gradient or mechanical efforts both on their static and dynamic properties [2–7]. The flow induced by temperature gradient in nematic hybrid oriented cell has been considered for the incompressible nematics in [3] and for the compressible ones in [7]. The flow in the cell inducing the temperature gradient across the nematic hybrid oriented film has been studied in [5]. The influence of the pretransition anomalies on the orientational processes in nematic hybrid oriented cell has been estimated in [6]. Above investigations deal with fixed geometry at the boundary surfaces and the non-sleeping [3,5,7] or the sleeping [6] boundary conditions for the velocity field. This paper elucidate the effect of the mechanical

Address correspondence to A. V. Zakharov, Saint Petersburg Institute for Machine Sciences, the Russian Academy of Sciences, Saint Petersburg 199178, Russia. E-mail: avz0911@yahoo.com; avak2vale@mail.ru

action on the one of the external surfaces of the nematic cell, which is expressed by the shear stress fixed at the boundary surface of the cell. New confinement produces the heat flow with the same temperature difference as it was done by previous results [3,5,7]. This paper considers the new mechanism of the temperature gradient initiation in hybrid aligned nematics.

This investigation is to show, in the framework of the classical Ericksen-Leslie theory [8–9], together with accounting for the thermoconductivity equation for the temperature field [10], the simple way how the external shear stress (SS)

$$(\sigma_{zx})_{z=d} = \sigma^0_{zx} \tag{1}$$

applied to the one boundary can build up the temperature gradient ∇T across the tumbling type hybrid aligned nematic (HAN) cell, and how much influences both the direction and magnitude of the hydrodynamic flow **v**, produced by the SS σ^0_{zx}, and that ∇T on the final director reorientation $\hat{\mathbf{n}}$ (t,**r**) across the LC cell.

Understanding how an elastic soft material, such as LCs, deforms under influence of the external forces, both a temperature gradient and mechanical efforts, is a question of great fundamental interest, as well as an essential piece of knowledge in material science. But taking into account that some LCs driven by shear flow display fascinating non equilibrium phenomena such as tumbling behaviour, that mechanical effort may, under certain conditions, overcome elastic, viscous, and thermomechanical forces, and cause a temperature gradient across the (initially isothermal) HAN cell [5].

Part.I. Basic equation for shear-induced reorientation process.

To fix ideas and notation, we shall considering a HAN film extends infinitely in two space directions (X and Y), and is delimited by two horizontal surfaces at mutial distance d (on scale of the order of 1 μm), with the σ^0_{zx} applied to the upper restricted boundary, and the temperature gradient between them given by ∇T(z) $\sim \Delta T/d$, is excited by the hydrodynamic flow **v**. Here $\Delta T = T_{up} - T_{lw}$, where the two subscribes up and lw refer to upper and lower boundary, respectively, and, of course, both temperatures fall within the nematic stability range. Assuming that the temperature gradient ∇T varies only in the z – direction, ∇T (z) $= \partial T(z)/\partial z\ \hat{\mathbf{k}}$, we can suppose that the components of the director $\hat{\mathbf{n}} = \sin\theta\hat{\mathbf{i}} + \cos\theta\hat{\mathbf{k}}$, as well as the rest of the physical quantities also depend only on the z – direction. Here θ denotes the polar angle, i.e., the angle between the direction of the director $\hat{\mathbf{n}}$ (t,**r**) and the normal $\hat{\mathbf{k}}$ to the boundary surfaces. The coordinate system defined by our task assumed that the director $\hat{\mathbf{n}}$ is in the XZ plane (or YZ plane), where $\hat{\mathbf{i}}$ is the unit vector directed parallel to the restricted surfaces, which coincides with the planar director orientation on the upper restricted surface ($\hat{\mathbf{i}} \parallel \hat{\mathbf{n}}_{z=d}$), and $\hat{j} = \hat{\mathbf{k}} \times \hat{\mathbf{i}}$. Therefore, the hybrid aligned nematic (HAN) state, where the upper surface of the LC cell is anchored homeotropically and the bulk of the cell contains a linear gradient in $\theta(z) = \pi/2dz$ from homeotropic orientation at the lower surface to planar orientation at the upper surface, i.e.,

$$\theta_{z=0} = 0, \theta_{z=d} = \frac{\pi}{2} \tag{2}$$

Taking into account that the size of the LC film d $\sim$ 1 μm, one can assume that the mass density ρ_m = const across the HAN cell, and one deals with an incompressible fluid. Incompressibility $\nabla \cdot \mathbf{v} = 0$, no-slip boundary condition $\mathbf{v}_{z=0} = 0$, and only the z – dependence together implies that only one nonzero component of the vector $\mathbf{v}$ exist, viz., $\mathbf{v}(t,z) = v_x(t,z)\hat{\mathbf{i}} = u(t,z)\,\hat{\mathbf{i}}$.

The hydrodynamic equations describing the reorientation of the LC phase confined between two solid surfaces, when to upper horizontal boundary is applied the SS σ^0_{zx}, and the temperature on the lower restricted surface is kept constant, whereas the heat flow vanishes or restricted on the upper boundary,

$$T_{z=0} = T_{lw}, \quad -\lambda_{\perp}\left(\frac{\partial T(z)}{\partial z}\right)_{z=d} = Q_0 \tag{3}$$

where $\lambda_{\perp}$ is the heat conductivity coefficient perpendicular to the director $\hat{\mathbf{n}}$, whereas Q_0 is the heat flow across the upper restricted surface, can be derived from the balance of elastic [1] $\mathbf{T}_{\mathrm{el}} = [-G(\theta)\theta_{zz} - 1/2G_{\theta}(\theta)\theta_z^2]\hat{\mathbf{j}}$, viscous [3,5–7] $\mathbf{T}_{\mathrm{vis}} = [\gamma_1\theta_t - A(\theta)u_z]\,\hat{\mathbf{j}}$, and thermomechanical [2,3,5–7] $\mathbf{T}_{\mathrm{tm}} = \xi\theta_z T_z(1/2 + \sin^2\theta)\,\hat{\mathbf{j}}$ torques, the Navier-Stokes equation for the velocity field $\mathbf{v}$, and the equation for the heat conduction, due to growth of the temperature difference ΔT on the LC cell boundaries, excited by the velocity field. Here $G(\theta) = K_1\sin^2\theta + K_3\cos^2\theta$, $A(\theta) = 1/2\ (\gamma_1 - \gamma_2\cos 2\theta)$, K_1 and K_3 are the splay and bend elastic constants of the LC phase, γ_1 and γ_2 are rotational viscosity coefficients (RVC), and $\xi \sim 10^{-12}$ J/m K is the thermomechanical constant [2,3,6]. In the following we are focused primarily on the heat conduction regime in the hybrid-oriented LC cell which assume that the temperature on the lower restricted surface is kept constant, whereas on the upper one the heat flow is vanished or restricted (Eq. (3)). Physically, this means that across the LC sample may built up of the temperature gradient ∇T, directed from the cooler to the warmer surfaces, under action of the hydrodynamic flow, excited by the SS σ^0_{zx} applied to the upper boundary.

To be able to observe the formation of the temperature difference ∇T across the LC sample, under action of the SS σ^0_{zx}, which initially was equal to zero, we consider the dimensionless analog both the linear and torque balance equations together with accounting for the the heat conduction equation in the form (The details of the derivation of these equations can be found in Ref. [3]., Eqs. (6)–(8))

$$\bar{\gamma}_1(\chi)\theta_\tau = \overline{A}(\theta)u_z + (\overline{G}(\theta)\theta_z)_z - \frac{1}{2}\overline{G}_\theta(\theta)\theta_z^2 - \delta_1\chi_z\theta_z\left(\frac{1}{2} + \sin^2\theta\right), \tag{4}$$

$$\delta_2\partial_\tau u(\tau, z) = \partial_z\bar{\sigma}_{zx}, \tag{5}$$

$$\overline{P}_z(\tau, z) + \frac{\partial R}{\partial\theta_\tau}\theta_z = 0, \tag{6}$$

$$\begin{aligned}\delta_3\partial_\tau\chi(\tau, z) = &\left[\chi_z(\lambda\cos^2\theta + \sin^2\theta)\right]_z + \\ &\delta_4\left[\chi\theta_z\left(\theta_\tau\left(\frac{1}{2} + \sin^2\theta\right) - u_z\sin^2\theta\left(1 + \frac{1}{2}\sin^2\theta\right)\right)\right]_z,\end{aligned} \tag{7}$$

where $\bar{\gamma}_1\ (\chi) = \gamma_1(\chi)/\gamma_{10}$, $\overline{A}\ (\theta) = A\ (\theta)/\gamma_{10}$, $\overline{G}\ (\theta) = G(\theta)/K_{10}$, $\bar{\sigma}_{zx} = \sigma_{zx}/\gamma_{10}$, $\sigma_{zx} = \delta R/\delta u_z = h(\theta)u_z - A(\theta)\theta_t - \xi T_z\theta_z\sin^2\theta(1 + 1/2\sin^2\theta)$ is the tangential component of the stress tensor σ_{ij} [3,5–7], R is the full Rayleigh dissipation function [3,11], $\overline{P} = d^2/K_{10}P$ is the dimensionless hydrostatic pressure in the HAN cell [3,11],

$\chi(t,z) = T(t,z)/T_{NI}$, and T_{NI} is the nematic-isotropic transition temperature, $\lambda = \lambda_{\|}/\lambda_{\perp}$, and $\lambda_{\|}$ and $\lambda_{\perp}$ are the heat conductivity coefficients parallel and perpendicular to the director $\hat{\mathbf{n}}$ [10]. Here γ_{10} and K_{10} are the highest values of the RVC $\gamma_1(\chi)$ and the splay constant $K_1(\chi)$ in the temperature interval $[\chi_1,\chi_2]$ belonging to the nematic phase, $t = (K_{10}/\gamma_{10}d^2)t$ is the dimensionless time, $z = z/d$ is the dimensionless distance away from the lower solid surface, $\delta_1 = \xi T_{NI}/K_{10}$, $\delta_2 = \rho_m K_{10}/\gamma_{10}^2$, $\delta_3 = \rho_m C_P K_{10}/(\gamma_{10}\lambda_{\perp})$ and $\delta_4 = \xi K_{10}/(\gamma_{10}\lambda_{\perp}d^2)$ are four parameters of the system [3,5–7]. Now the dimensionless temperature field $\chi(t,z)$ in the LC film confined between two solid surfaces, when the temperature on the lower surface is kept constant, whereas on the upper assumed that the heat flow is vanished or restricted, must satisfy the boundary conditions

$$\chi(z)_{z=0} = \chi_1, (\chi(z)/z)_{z=1} = q_0 \tag{8}$$

where $q_0 = -Q_0 d/T_{NI}\lambda_{\perp}$ is the dimensionless heat flow across the upper restricted surface. On the other hand, when the director $\hat{\mathbf{n}}$ is strongly homeotropically anchored to the lower and homogeneously to the upper restricted surfaces the polar angle has to satisfy the boundary conditions

$$\theta(z)_{z=0} = 0, \theta(\mathrm{z})_{\mathrm{z}=1} = \frac{\pi}{2}, \tag{9}$$

and its initial orientation is perturbed parallel to the interface, with $\theta(t = 0,z) = \pi/2$, and then, under action of the SS σ_{zx}^0, allowed to relax to its equilibrium value $\theta_{eq}(z)$. The velocity on the lower surface must satisfy the no-slip boundary condition

$$u(z)_{z=0} = 0, \tag{10}$$

whereas on the upper surface the SS is applied as

$$(\sigma_{zx})_{z=1} = \sigma_{zx}^0. \tag{11}$$

For the case of 4-cyano-4′-octylbiphenyl ~(8CB), at temperature corresponding to nematic phase, the set of parameters, which involved in Eqs. (4)–(7), are $\delta_1 \sim 24$, $\delta_2 \sim 2\ 10^{-6}$, $\delta_3 \sim 6\ 10^{-4}$, and $\delta_4 \sim 10^{-10}$ (for details, see Ref. [6]). Using the fact that δ_2, δ_3, and δ_4 are all << 1, the Navier-Stokes (Eq. (5)) and the heat conduction Eq. (7) equations can be considerably simplified. Thus, the whole left-hand side of Eqs. (5) and (7) can be neglected and these equations takes the form

$$\bar{\sigma}_{zx} = h(\theta)u_z - A(\theta)\theta_\tau - \delta_1\chi_z\theta_z\sin^2\theta\left(1 + \frac{1}{2}\sin^2\theta\right) = \sigma_{zx}^0, \tag{12}$$

$$[\chi_z(\lambda\cos^2\theta + \sin^2\theta)]_z = 0. \tag{13}$$

The onset of a temperature difference $\Delta\chi(t,z)$ across the LC cell under action of the SS σ_{zx}^0 can be described by the equation

$$\chi_z = \frac{q_0}{\lambda\cos^2\theta + \sin^2\theta}. \tag{14}$$

Physically, this means that the temperature field χ(t,z) across the HAN cell, under abovementioned conditions, is proportional to the heat flow q_0 on the upper restricted surface, when the temperature on the lower surface is kept constant.

Part. II Shear-induced reorientation simulation.

The relaxation of the director $\hat{\mathbf{n}}$ to its equilibrium orientation $\hat{\mathbf{n}}_{eq}$, is described by the evolution of its polar angle θ(t,z) from the initial condition $\theta(t=0,z)=\pi/2$ to θ_{eq}(z). This has been calculated by solving of the system of the nonlinear partial differential equations (4), (5), (12), and (14), together with the boundary conditions (8), (9), (10), and (11), by means of the numerical relaxation method [12], and results, at different times, are shown in Figure 1: $\tau_1=0.001$ [curve (1)], ..., $\tau_7=\tau_R$[curve (7)], when the dimensionless heat flow is $q_0=0.02(Q_0\sim 200\,\mathrm{nW}/\mu\mathrm{m}^2)$, for a number of values of the SS $\sigma^0_{zx}=10(\sim 5\,\mathrm{Pa})$ Figure 1(a), with the value of the relaxation time τ_R $(\sigma^0_{zx}=10)=0.4$ ($\sim$0.07s), 20($\sim$10 Pa) Figure 1(b), with τ_R $(\sigma^0_{zx}=20)=0.32(\sim 0.05\mathrm{s})$, and 30($\sim$15 Pa) Figure 1(c), with $\tau_R(\sigma^0_{zx}=30)=0.6$ ($\sim$0.1s), respectively, directed in the positive direction. The relaxation criterion $\varepsilon=|(\theta_{m+1}\ (t,z)-\theta_m(t,z))/\theta_m(t,z)|$ for calculating procedure was chosen equal to be 10^{-4}, and the numerical procedure was then carried out until a prescribed accuracy was achieved. Here m is the iteration number. According to our calculations, the SS σ^0_{zx} produces the velocity field u(t,z) directed in the positive direction, and it effects on the director distribution across the LC cell so strong, that in the middle part of the LC cell the biggest value of the polar angle is equal to 5.5 ($\sim$315°), and the director executes, practically, a full cycle of rotation (see, Fig. 1(c)). That influence decrease with decreasing of σ^0_{zx}.

Physically, this means that the hydrodynamic torque $\mathbf{T}_{vis}$ acting on the unit volume of the LC phase, in the case of $|\gamma_1|>|\gamma_2|$, produces a tumbling regime, which is

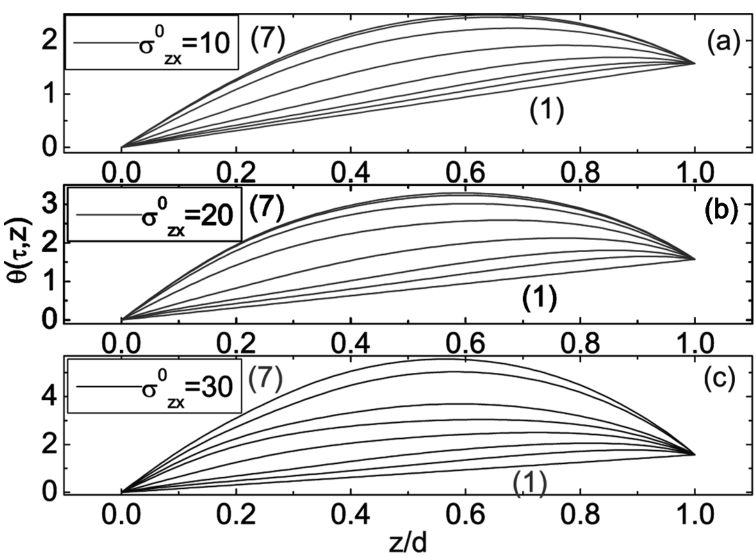

Figure 1. (a) The polar angle θ(t,z)$\sim$(in rad) vs. distance z/d away from the lower restricted surface under influence of the SS $\sigma^0_{zx}=10(\sim 5\,\mathrm{Pa})$, directed in the positive direction, at different times $\tau_1=0.001\sim$(curve (1)), and $\tau_R=\tau_7=0.4(\sim 0.07\mathrm{s})$, whose values increase from curve (1) to curve (7), when the dimensionless heat flow across the upper boundary is $q_0=0.02$ ($Q_0\sim$ 200 nW/μm^2). (b) and (c) the same as in (a), but SS $\sigma^0_{zx}=20(\sim 10\,\mathrm{Pa})$, $\tau_R=0.32(\sim 0.053\mathrm{s})$ and 30($\sim$15 Pa), $\tau_R=0.6(\sim 0.1\mathrm{s})$, respectively.

characterized by a continuous rotation of the director in the shear plane. But taking into account that the director field is strongly anchored to both surfaces, homeotropically to the lower and homogeneously to the upper, the balance of the elastic, hydrodynamic, and thermomechanic forces leads to rotation of the director field mainly in the middle part of the LC cell. The relaxation process of the velocity field is characterized by the growth of u(t,z) upon increasing t, before getting to the equilibrium distribution $u_{eq}(z)$ across the LC cell (see, Fig. 2). The distribution is characterized by the maximum on the upper bounding surface, and the hydrodynamic flow is directed parallel to both boundaries in the positive direction. The maximum of the absolute magnitude of the dimensionless velocity $u_{eq}(z) = (\gamma_{10}d/K_{10})v_x^{eq}(z)$ in the HAN cell, at the final stage of the relaxation process is equal to 25($\sim$787 μm/s), at $\sigma^0_{zx} = 10$ (Fig. 2(a)), 75($\sim$2266 μm/s), at $\sigma^0_{zx} = 20$ (Fig. 2(b)), and 95($\sim$2871 μm/s), at $\sigma^0_{zx} = 30$ (Fig. 2(c)), respectively. In the case when the heat flow across the upper surface is restricted ($q_0 = 0.02$ ($Q_0 \sim 200\,\mathrm{nW}/\mu\mathrm{m}^2$)), one deals with a practically linear increase of χ(t,z) across the LC cell from the temperature on the bottom $\chi_{z=0} = \chi_{lw} = 0.98(\sim 307\,\mathrm{K})$ surface to the temperature on the top $\chi_{z=1} = \chi_{up}$ surface. The relaxation of the dimensionless temperature on the upper restricted surface $\chi_{z=1}(t)$ to its equilibrium value $\chi^{eq}_{z=1}$, at three different values of SS $\sigma^0_{zx} = 10$, 20 and 30 is shown in Figure 3. Calculations shows that under influence of the lower SS $\sigma^0_{zx} = 10$ and higher $\sigma^0_{zx} = 30$, the relaxation process of the temperature field is characterized practically the same values of $\chi^{eq}_{z=1} : \chi^{eq}_{z=1}(\sigma^0_{zx} = 10) \sim 0.995(\sim 311.5\,\mathrm{K})$ and $\chi^{eq}_{z=1}(\sigma^0_{zx} = 30) \sim 0.9946(\sim 311.3\,\mathrm{K})$, whereas in the case of $\sigma^0_{zx} = 20$ the dimensionless temperature on the upper restricted surface is equal to $\sim$0.992($\sim$310.6 K). Note that in all these cases the dimensionless temperature on the lower restricted surface is kept constant $\chi_{z=0} = \chi_{lw} \sim 0.98(\sim 307\,\mathrm{K})$, and across the LC sample built up of the vertical temperature gradient ∇T directed to the warmer upper boundary. So, the highest temperature difference $\Delta\chi = \chi_{up} - \chi_{lw} = 0.015(\sim 4.5\,\mathrm{K})$, which initially was equal to zero, build up in the LC sample under influence of the lower SS $\sigma^0_{zx} = 10$.

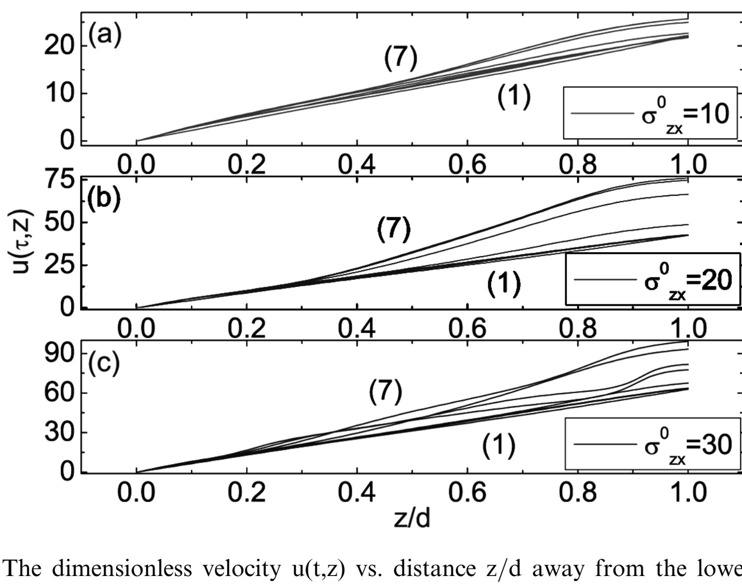

Figure 2. The dimensionless velocity u(t,z) vs. distance z/d away from the lower to upper restricted surfaces, at different times, the same as in Figure 1.

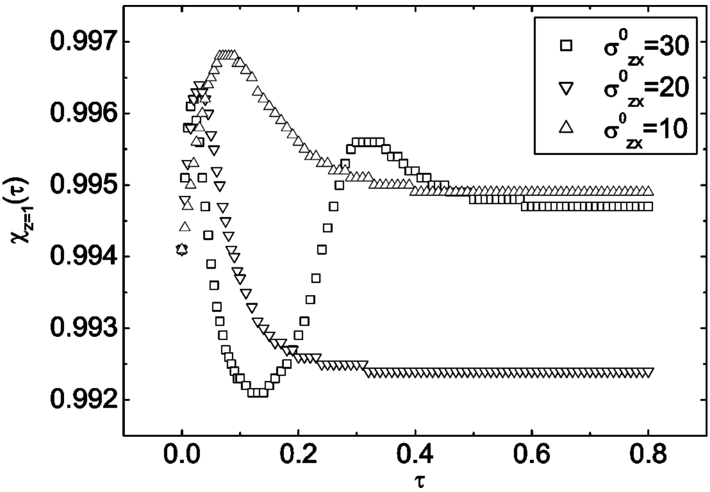

Figure 3. Plot of relaxation of the dimensionless temperature on the upper restricted surface $\chi_{z=1}(t)$ to its equilibrium value $\chi^{eq}_{z=1}$, at three values of the SS $s^0_{zx} = 10(\sim 5\,Pa)$, $20(\sim 10\,Pa)$, and $30(\sim 15\,Pa)$, respectively, directed in the positive direction, whereas on the lower restricted surface the temperature is kept $\chi_{z=0} = 0.98$.

The effects of the SS σ^0_{zx} directed in the negative direction both on the director $\hat{\mathbf{n}}$ reorientation to its equilibrium orientation $\hat{\mathbf{n}}_{eq}$ and the velocity field u(t,z), which excited by the SS σ^0_{zx}, are shown in Figures 4 and 5, respectively. The relaxation of the director is described by the evolution of its polar angle θ(t,z) from the initial condition $\theta(t=0,z)=\pi/2$ to $\theta_{eq}(z)$, and results, at different times, are shown in Figure 4: $\tau_1 = 0.001$ [curve (1)], ..., $\tau_7 = \tau_R$[curve (7)], when the dimensionless heat flow is $q_0 = 0.02$ ($Q_0 \sim 200\,nW/\mu m^2$), for a number of values of the SS $\sigma^0_{zx} = -10(\sim -5\,Pa)$ Figure 4(a), with the value of the relaxation time $\tau_R(\sigma^0_{zx} = -10) = 0.64(\sim 0.11s)$, $-20(\sim -10\,Pa)$ Figure 4(b), with $\tau_R(\sigma^0_{zx} = -20) = 0.47(\sim 0.08s)$, and $-30(\sim -15\,Pa)$ Figure 4(c), with t_R $(\sigma^0_{zx} = -30) = 0.48(\sim 0.08s)$, respectively, directed in the negative direction.

According to our calculations, the SS σ^0_{zx} produces the velocity field u(t,z) directed in the negative direction, and it effects on the director distribution across the LC cell so strong, that in the middle part of the LC cell the director field n is directed, practically, orthogonal to both boundaries (the biggest value of the polar angle is equal to $3.14(\sim 180°)$(see, Fig. 4). That influence increase with increasing of $|\sigma^0_{zx}|$. The relaxation process of the velocity field is characterized by the growth of |u(t,z)| upon increasing t, before getting to the equilibrium distribution $u_{eq}(z)$ across the LC cell (see, Fig. 5). The distribution is characterized by the maximum on the upper bounding surface, and the hydrodynamic flow is directed parallel to both boundaries in the negative direction. The maximum of the absolute magnitude of the dimesionless velocity $u_{eq}(z) = (\gamma_{10} d/K_{10} v^{eq}_x(z)$ in the HAN cell, at the final stage of the relaxation process is equal to $33(\sim 1007\,\mu m/s)$, at $\sigma^0_{zx} = -10$ (Fig. 5(a)), $60.4(\sim 1861\,\mu m/s)$, at $\sigma^0_{zx} = -20$ (Fig. 5(b)), and $102(\sim 3142\,\mu m/s)$, at $\sigma^0_{zx} = -30$ (Fig. 5(c)), respectively. In the case when the heat flow across the upper surface is restricted ($q_0 = 0.02$ ($Q_0 \sim 200\,nW/\mu m^2$)), one also deals with a practically linear increase of χ(t,z) across the LC cell from the temperature on the bottom $\chi_{z=0} = \chi_{lw} = 0.98(\sim 307\,K)$ surface to the temperature on the top $\chi_{z=1} = \chi_{up}$ surface. The relaxation of the dimensionless

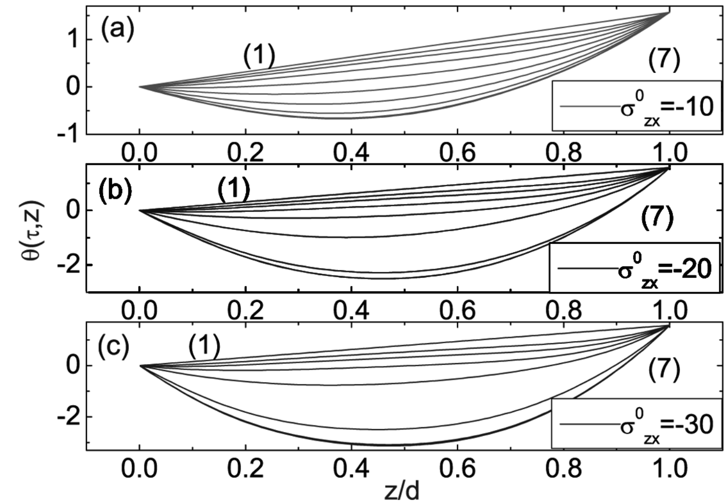

Figure 4. (a) The polar angle $\theta(t,z) \sim$ (in rad) vs. distance z/d away from the lower restricted surface under influence of the SS $\sigma^0_{zx} = -10(\sim -5\,\text{Pa})$, directed in the negative direction, at different times $\tau_1 = 0.001 \sim$ (curve (1)), and $\tau_R = \tau_7 = 0.64(\sim 0.11\text{s})$, whose values increase from curve (1) to curve (7), when the dimensionless heat flow across the upper boundary is $q_0 = 0.02(Q_0 \sim 200\text{nW}/\mu\text{m}^2)$. (b) and (c) the same as in (a), but SS $\sigma^0_{zx} = -20(\sim -10\,\text{Pa})$, $\tau_R = 0.47(\sim 0.08\text{s})$ and $-30(\sim -5\,\text{Pa})$, $\tau_R = 0.48(\sim 0.08\text{s})$, respectively.

temperature on the upper restricted surface $\chi_{z=1}(t)$ to its equilibrium value $\chi^{eq}_{z=1}$, at three different values of SS $\sigma^0_{zx} = -10$, -20, and -30 is shown in Figure 6. Calculations shows that the relaxation process of $\chi_{z=1}$ (t) to its equilibrium value $\chi^{eq}_{z=1}$, at both lower values of the SS $\sigma^0_{zx} = -20$ and -30, is characterized by oscillating behaviour of $\chi_{z=1}$ (t), before getting to $\chi^{eq}_{z=1}$ $(\sigma^0_{zx} = -20) = 0.9945$ ($\sim$311.3 K) and $\chi^{eq}_{z=1}$

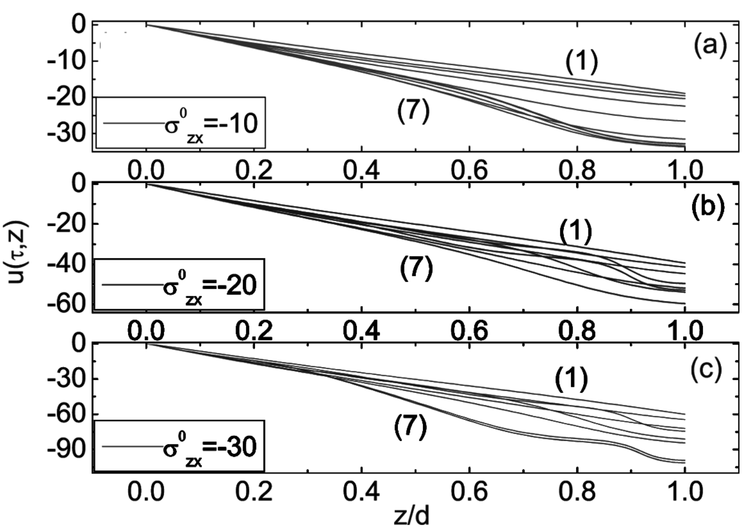

Figure 5. The dimensionless velocity u(t,z) vs. distance z/d away from the lower to upper restricted surfaces, at different times, the same as in Figure 4.

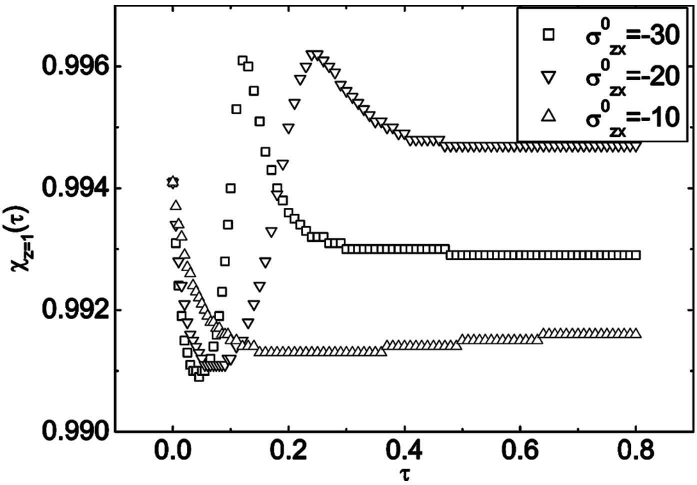

Figure 6. Plot of relaxation of the dimensionless temperature on the upper restricted surface $\chi_{z=1}$ (t) to its equilibrium value $\chi^{eq}_{z=1}$, at three values of the SS $\sigma^0_{zx} = -10(\sim -5\,\text{Pa}), -20(\sim -10\,\text{Pa})$, and $-30(\sim -15\,\text{Pa})$, respectively, directed in the negative direction, whereas on the lower restricted surface the temperature is kept $\chi_{z=0} = 0.98$.

$(\sigma^0_{zx} = -30) = 0.993$ ($\sim$310.8 K), respectively, whereas $\chi^{eq}_{z=1}$ $(\sigma^0_{zx} = -10)$ is equal to 0.992 ($\sim$310.4 K). So, the highest temperature difference $\Delta\chi = 0.015$ ($\sim$4.3 K), which initially was equal to zero, built up in the HAN sample, under influence of the SS $\sigma^0_{zx} = -20(\sim -10\,\text{Pa})$. Note that in all these cases the dimensionless temperature on the lower restricted surface is kept constant $\chi_{z=0} = \chi_{lw} \sim 0.98$ ($\sim$307 K), and across the LC sample built up of the vertical temperature gradient ∇T directed to the warmer upper boundary.

It should be pointed out that the normal components σ_{ii}(i = x,z) of the stress tensor does not alter the internal director redistribution in the HAN cell because σ_{ii} (i = x,z) contribute nothing in the balance of the linear momentums.

Conclusions

To summarize, our theoretical results demonstrate that the shear stress applied to the upper restricted surface of the tumbling type hybrid-oriented liquid crystal cell, when the director is strongly anchored to both restricted surfaces, homeotropically to the lower and homogeneously to the upper, may, under certain conditions, overcome elastic, viscous and thermomechanical forces, and cause a temperature gradient across the studied liquid crystal film, with the maximum absolute value of the temperature difference $\Delta T = T_{up(lw)} - T_{lw(up)}$ ranging up to a few degrees. That shear stress can produce a temperature gradient only in the conduction regime, assuming that the temperature on the lower (upper) surface is kept constant, whereas the heat flow across the other surface is restricted. It has been also shown that the highest temperature difference ΔT, which initially was equal to zero, may built up in the HAN sample, under influence of the shear stress effort directed both in the positive and negative directions. Notes that the mechanical mechanism, which provides formation of a temperature gradient across the studied HAN film, can potentially be used in the biological and chemical analysis and synthesis.

References

[1] de Gennes, P. G., & Prost, J. (1995). *The Physics of Liquid Crystals*, Oxford University Press: Oxford, UK.
[2] Akopyan, R. S., & Zeldovich, B. Ya. (1984). *JETP*, *60*, 953.
[3] Zakharov, A. V., & Vakulenko, A. A. (2007). *J. Chem. Phys.*, *127*, 084907.
[4] Dequidt, A., & Oswald, P. (2007). *Euro. Phys. Lett.*, *80*, 26001.
[5] Zakharov, A. V., & Vakulenko, A. A. (2008). *Chem. Phys. Lett.*, *454*, 80.
[6] Zakharov, A. V., Vakulenko, A. A., & Romano, S. (2008). *J. Chem. Phys.*, *128*, 074905.
[7] Zakharov, A. V., & Vakulenko, A. A. (2009). *Phys. Rev.*, *E79*, 011708.
[8] Ericksen, J. L. (1960). *Arch. Ration. Mech. Anal.*, *4*, 231.
[9] Leslie, F. M. (1968). *Arch. Ration. Mech. Anal.*, *28*, 265.
[10] Landau, L. D., & Lifshitz, E. M. (1987). *Fluid Mechanics*, Pergamon Press: Oxford, UK.
[11] Stewart, I. W. (2004). *The Static and Dynamic Continuum Theory of Liquid Crystals*, Taylor and Francis: London, UK.
[12] Berezin, I. S., & Zhidkov, N. P. (1965). *Computing Methods*, Pergamon Press: Oxford, UK.